Nucleic Acids Research, 1999, Vol. 27, No. 6 **1473–1479**

Mutational analysis of the antigenomic *trans*-acting *delta* ribozyme: the alterations of the middle nucleotides located on the P1 stem

Sirinart Ananvoranich, Daniel A. Lafontaine and Jean-Pierre Perreault*

Département de Biochimie, Faculté de Médecine, Université de Sherbrooke, Sherbrooke, Québec J1H 5N4, Canada

Received November 12, 1998; Revised and Accepted January 20, 1999

ABSTRACT

Our previous report on *delta* ribozyme cleavage using a *trans*-acting antigenomic *delta* ribozyme and a collection of short substrates showed that the middle nucleotides of the P1 stem, the substrate binding site, are essential for the cleavage activity. Here we have further investigated the effect of alterations in the P1 stem on the kinetic and thermodynamic parameters of *delta* ribozyme cleavage using various ribozyme variants carrying single base mutations at putative positions reported. The kinetic and thermodynamic values obtained in mutational studies of the two middle nucleotides of the P1 stem suggest that the binding and active sites of the *delta* ribozyme are uniquely formed. Firstly, the substrate and the ribozyme are engaged in the formation of a helix, known as the P1 stem, which may contain a weak hydrogen bond(s) or a bulge. Secondly, a tertiary interaction involving the base moieties in the middle of the P1 stem likely plays a role in defining the chemical environment. As a consequence, the active site might form simultaneously or subsequently to the binding site during later steps of the pathway.

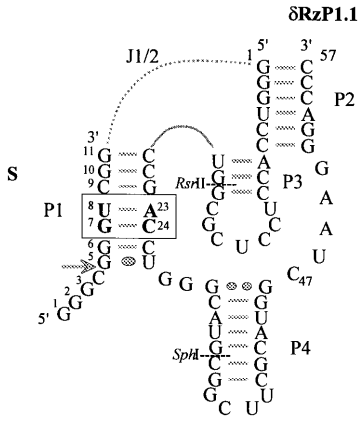

Figure 1. Secondary structure of the engineered *trans*-acting antigenomic *delta* ribozymes and their complementary substrates. The base paired regions of the pseudoknot-like structure are numbered according to Perrotta and Been (5). The secondary structure of the complex formed between δRzP1.1 and its substrate, SP1.1, is shown. The arrow indicates the cleavage site. The nucleotide numbering of both the substrate and ribozyme is indicated and referred to throughout the text. The mutational analyses were carried on positions 7 and 8 of the substrate and positions 23 and 24 of the ribozyme.

INTRODUCTION

Delta ribozymes, derived from the genome of hepatitis *delta* virus (HDV), are metalloenzymes. Like other catalytically active ribozymes, namely hammerhead and hairpin ribozymes, the *delta* ribozymes cleave a phosphodiester bond of their RNA substrates and give rise to reaction products containing a 5′-hydroxyl and a 2′,3′-cyclic phosphate termini. Two forms of *delta* ribozymes, namely genomic and antigenomic, were derived and referred to by the polarity of HDV genome from which the ribozyme was generated. Both *delta* ribozyme forms exhibit self-cleavage activity and it has been suggested that they are involved in the process of viral replication (1). This type of activity has been described as *cis*-acting *delta* ribozymes (2).

Previously we have described the kinetics and the substrate specificity of a *trans*-acting antigenomic *delta* ribozyme, which is composed of 57 nt derived from the antigenomic self-cleaving motif, and its substrate is 11 nt long (Fig. 1; 3,4). Despite the same substrate recognition sequence, *trans*-acting antigenomic *delta* ribozyme systems, generated by a similar approach in the elimination of the J1/2 portion, are of different lengths, ranging from 52 to 80 nt long, and exhibit various kinetic values (5–8). It has been previously discussed that the differences were results of the variation in the non-ribozyme flanking sequences (4,5). In our previous report on the substrate specificity, we studied the interactions between the *delta* ribozyme and the substrate, which are generally accepted as the formation of a helix referred to as the P1 stem (Fig. 1). We introduced a single mutation into each individual nucleotide of the substrate (positions 5–11 of the substrate) and showed that the base pairs in the middle of the P1 stem (corresponding to A23 and C24 of the *delta* ribozyme) are important not only for substrate binding, but also for subsequent steps in the cleavage pathway, including chemical cleavage (3).

Recently, the crystal structure of a self-cleaving genomic *delta* ribozyme has been reported to have a putative active site buried in a unique nested double pseudoknot without any indication of

*To whom correspondence should be addressed. Tel: +1 819 564 5310; Fax: +1 819 564 5340; Email: jperre01@courrier.usherb.ca

the involvement of the nucleotides located on the P1 stem (9). Regardless of the similar predicted secondary structures of genomic and antigenomic *delta* ribozymes (2), it is possible that the X-ray structure of both *delta* ribozymes are different. More studies are required to achieve a better understanding of the native structure of antigenomic and genomic *delta* ribozymes, especially for their *trans*-active versions. In order to elaborate the effect of the P1 stem sequence on the cleavage pathway, we performed a detailed kinetic analysis of the wild-type *delta* ribozyme (δRzP1.1) and six of its variants (three δRzP1-A23N and three δRzP1-C24N ribozymes). Comparative analysis using both kinetic and thermodynamic parameters in this report further confirms the presence of tertiary interactions involving the positions A23 and C24 in defining the chemical environment of the *trans*-acting antigenomic *delta* ribozyme and its substrate complex.

MATERIALS AND METHODS

Preparation of RNAs

Ribozymes and substrates were synthesized using T7 RNA polymerase as described previously (3). Uncleavable substrate analogs having a deoxyribonucleotide substitution at position 4 were chemically synthesized by the Keck Oligonucleotide Synthesis Facility (Yale University), deprotected as described by Perreault and Altman (10) and purified on 20% denaturing PAGE gels. Substrates were end-labeled by T4 polynucleotide kinase as described previously (3). The presence of alternative forms of ribozymes and substrates were examined using a non-denaturing gel electrophoresis system. Various concentrations of ribozymes and/or substrates within the range used in these experiments were electrophoresed on 12% non-denaturing polyacrylamide gels using 29:1 acrylamide:bis-acrylamide in 45 mM Tris–borate, pH 7.5, and 10 mM $MgCl_2$ buffer and the relative amounts of the various forms quantified using a phosphorimaging screen and a Molecular Dynamics radioanalytic scanner.

Kinetic analysis

Pseudo first-order cleavage rate constants (k_2 and K_m') were measured with an excess of ribozyme (5–600 nM) and trace amounts of 5′-^{32}P-end-labeled substrate (<0.1 nM). Unless otherwise stated, the reactions were carried out under standard conditions in 20 µl mixtures containing 50 mM Tris–HCl, pH 7.5, and 10 mM $MgCl_2$ and were incubated at 37°C. At least two independent experiments were performed for each measurement. Reaction rates (k_{obs}) were obtained from fitting the experimental data to the equation $A_t = A_\alpha(1 - e^{-kt})$ where A_t is the percentage of cleavage at time t, A_α is the maximum cleavage (or the end point of cleavage) and k is the reaction rate.

Rates of substrate dissociation (k_{-1}) were measured by pulse–chase experiments. Partitioning experiments as described by Hertel *et al.* (11) and Fedor and Uhlenbeck (12) were performed with a slight modification. An inactive version of the ribozyme, which contains the substitution of A for C at position 47 in the wild-type ribozyme, was assumed to have similar substrate binding and dissociation properties as an active ribozyme. Trace amounts of end-labeled substrate were mixed with an inactive ribozyme (250 nM–1 µM) to form an enzyme–substrate complex. After an initial binding period (10 s–5 min), the initial mixture (3 µl) was added to 27 µl of the active ribozyme. The concentration of active ribozyme during the chase period ranged from 2 to 20 µM, or 8–80 times the concentration of the inactive ribozyme. The observed rate of cleavage was obtained from fitting the experimental data describing the substrate left during the chase period to a pseudo first-order equation as mentioned earlier. The observed cleavage rate (k_{obs}) in the pulse–chase reactions corresponds to the rate of cleavage (k_2) and the rate of substrate dissociation (k_{-1}), i.e. $k_{obs} = k_2 + k_{-1}$. Control experiments were carried out by adding trace amounts of end-labeled substrate to a solution containing both inactive and active ribozymes at the same concentrations as in the test experiments. Observed cleavage rates were similar to those obtained from parallel reactions containing only active ribozyme. This observation indicated that the concentrations of active ribozyme were high enough to prevent the reassociation of the substrate to the inactive ribozyme during the chase period, reflecting the rate of cleavage (k_2).

Rates of substrate association (k_1) were calculated from the equation described for the equilibrium state of the substrate dissociation ($K_d^S = k_{-1}/k_1$).

Equilibrium dissociation constants of both the substrate and the product (K_d^S and K_d^P) were measured by non-denaturing PAGE. Substrate analogs and reaction products were chemically synthesized so as to have sequences corresponding to the P1 stem of the cleavable complementary substrates. For the uncleavable substrate analog, the ribose was substituted by the 2′-deoxyribose moiety at position 4, resulting in an uncleavable substrate. For example, for the wild-type substrate SP1.1, SdC4 was synthesized as GGGdC_4GGGUCGG. Various ribozyme concentrations (5–1000 nM) were individually mixed with trace amounts of end-labeled substrate analog (<0.1 nM) under similar cleavage assay conditions. To achieve an equilibrium state, the mixtures were incubated at 37°C for 1 h prior to fractionation on 12% acrylamide non-denaturing gels. The values of K_d^S were calculated by fitting experimental data to the simple binding equation (% bound substrate = $[RZ]/K_d + [RZ]$, where [RZ] is the concentration of ribozyme and K_d is the equilibrium dissociation constant). K_d^P values were determined in the same manner using the labeled 3′-reaction products.

RESULTS

Delta ribozyme variants and their complementary substrates

The *trans*-acting *delta* ribozyme variants were produced using plasmid pδRzP1.1 (3,4). The variants have either A23 or C24 mutated to one of the other three possible bases. The six resulting *delta* ribozyme variants are named for the altered nucleotide (δRzP1-A23C, -A23G, -A23U, -C24A, -C24G and -C24U; Table 1). Complementary or compensatory substrates (Table 1) were generated in which either position 7 or 8 of the wild-type substrate (SP1.1) was altered in order to restore the Watson–Crick base pair formation of the P1 stem between the substrates and the ribozyme variants. Prior to performing a kinetic analysis, native gel electrophoresis was used to test for the possible presence of alternative forms of the transcripts as described in Materials and Methods. No alternative conformers were detected within the concentration range used (0.1–600 nM) when individual transcripts were tested.

Primarily, we assessed the cleavage activity of each variant and compared its extent of cleavage with that of the wild-type ribozyme, δRzP1.1 (Fig. 2). Despite the different cleavage rates

Table 1. Sequences of transcripts used

Transcripts	Sequence
Substrates	
SP1.1	$_{1}$GGGCGGGUCGG$_{11}$
SG7A	GGGCGGAUCGG
SG7C	GGGCGGCUCGG
SG7U	GGGCGGUUCGG
SU8A	GGGCGGGACGG
SU8C	GGGCGGGCCGG
SU8G	GGGCGGGGCGG
SU8G-9mers	$_{1}$GCGGGGCGG$_{9}$
Products	
PP1.1	$_{5}$GGGUCGG$_{11}$
P2G7A	GGAUCGG
P2G7C	GGCUCGG
P2G7U	GGUUCGG
P2U8A	GGGACGG
P2U8C	GGGCCGG
P2U8G	GGGGCGG
Ribozymes	
δRzP1.1	$_{20}$CCGACCU$_{26}$
δRzP1-A23C	CCGCCCU
δRzP1-A23G	CCGGCCU
δRzP1-A23U	CCGUCCU
δRzP1-C24A	CCGAACU
δRzP1-C24G	CCGAGCU
δRzP1-C24U	CCGAUCU

Subscript numbers represent nucleotide positions corresponding to the substrates, the reaction products and the ribozymes (as depicted in Fig. 1).

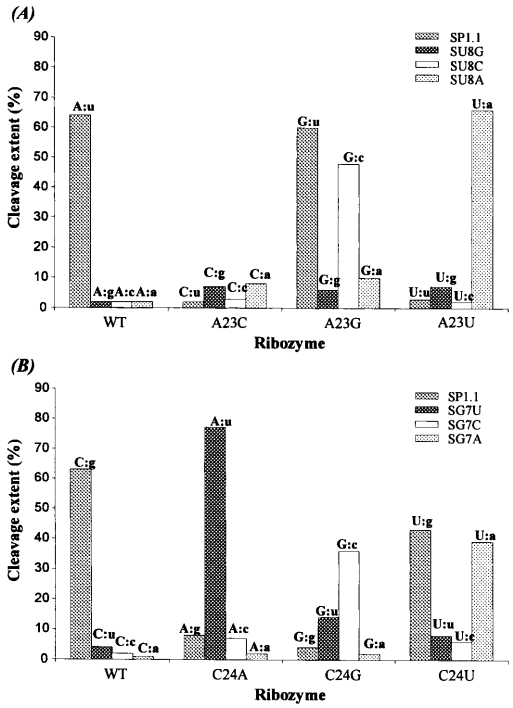

Figure 2. Comparative analyses of the cleavage reactions catalyzed by *delta* ribozymes. The extents of cleavage of the δRzP1-A23N ribozyme variants were compared with that of the wild-type ribozyme, δRzP1.1 (**A**). The extents of cleavage of the δRzP1-C24N ribozyme variants were compared with that of the wild-type (**B**). The base pair formed between the ribozyme and the substrate is indicated by the capital and lower case letters, respectively, on each bar of the histogram. The values are an average calculated from at least two independent experiments.

observed, the extents of cleavage were observed to be between 0 and 80%, as compared with 60% for the wild-type ribozyme. Under single turnover conditions, δRzP1.1 is unable to cleave substrates with a mismatch at either position 7 or 8 reported previously (3). Ribozyme variants exhibited wider ranges of substrate specificity when G or U was introduced at either A23 or C24 of δRzP1.1. For example, δRzP1-A23G could cleave its complementary substrate (SU8C) as efficiently as the wild-type substrate (SP1.1) and cleaved SU8A with less efficiency. δRzP1-C24U cleaved single mismatched substrates (i.e. SP1.1, SG7U and SU7C). In contrast, δRzP1-C24A, having A substituted for C24, specifically cleaved only its complementary substrate, SG7U. Interestingly, δRzP1-A23C, which has C substituted for A23, did not efficiently cleave either its complementary substrate (SU8G) or any single mismatched substrates (i.e. SP1.1, SU8C and SU8A). In order to eliminate possible alternative forms of SU8G–ribozyme occurring due to two repeated GGGC sequences in SU8G, the SU8G-9mer was synthesized with only 2 nt (GC) adjacent to the cleavage site instead of the usual 4 nt (Table 1). This shorter version of SU8G was weakly cleaved by δRzP1-A23C, with only a maximum cleavage extent of 7% after 4 h incubation. In order to determine what might cause this weak catalytic activity, various concentrations of δRzP1-A23C were pre-incubated with trace amounts of either end-labeled SU8G or SU8G-9mer and subjected to non-denaturing gel electrophoresis. Alternative conformers were detected when δRzP1-A23C was incubated with SU8G (11 nt), but not with SU8G-9mer. We also verified the effect of magnesium on the δRzP1-A23C cleavage of SU8G-9mer by increasing the magnesium concentration above the 10 mM used under standard assay conditions (data not shown). Even after 3.5 h of incubation, a maximum cleavage extent of 15% was detected in the presence of 25 mM magnesium. However, at $MgCl_2$ concentrations >100 mM, we observed an inhibitory effect of the magnesium on δRzP1-A23C cleavage activity.

Non-denaturing gel electrophoresis was also used for determining the binding affinity of δRzP1-A23C and -A23U for their uncleavable substrates (i.e. SP1.1 and SU8C; see Table 2), since δRzP1.1 was reported to bind its uncleavable substrates containing a single mutation at position 8 with the same affinity as the wild-type substrate (3). Similar phenomena were observed for the A23N ribozyme variants with their uncleavable substrates (Table 2). δRzP1-A23C could bind its complementary substrate analog with a K_d^S of 36 nM and the uncleavable substrates SP1.1 and SU8C with K_d^S of 33 ± 8 and 25 ± 8 nM, respectively. δRzP1-A23U could bind to its complementary substrate analog with K_d^S of 113 nM and SP1.1 as well as SU8C with K_d^S of 34 ± 3 and 140 nM, respectively. Since the δRzP1-C24N variants exhibited wider substrate specificities than those with the mutation at position A23, their substrate binding affinity was not determined.

Kinetic studies of *delta* ribozyme variants

The kinetic studies were employed to determine the effect of altering the P1 stem sequence on the cleavage pathway. The values of substrate association (k_1) and dissociation (k_{-1}),

Table 2. Kinetic parameters for *delta* ribozymes

Ribozyme	k_2 (min^{-1})	K_m' (nM)	k_2/K_m (μM^{-1} min^{-1})	K_{Mg} (mM)	K_d^S (nM)	K_d^P (nM)	Calculated K_d^{P1} (nM)	k_{-1} (min^{-1})	Calculated k_1 ($\mu M^{-1}min^{-1}$)
δRzP1.1	0.34 ± 0.02	17.9 ± 5.6	19	2.2 ± 1	32 ± 3	42 ± 5	28.5	0.13 ± 0.03	4.0
δRzP1-A23C[a]	0.097 ± 0.01	15.5 ± 0.9	6	[b]-	36 ± 5	45 ± 6	1.3	ND	ND
δRzP1-A23G	0.056 ± 0.01	14.8 ± 6.4	4	5.8 ± 1	36 ± 4	74 ± 9	1.3	ND	ND
δRzP1-A23U	0.19 ± 0.01	2.5 ± 0.4	76	1.9 ± 1.2	113 ± 20	17 ± 3	25.6	0.02 ± 0.01	0.17
δRzP1-C24A	0.26 ± 0.02	102 ± 13	3	2.4 ± 1	164 ± 22	648 ± 22	734.5	0.02 ± 0.01	0.12
δRzP1-C24G	0.23 ± 0.02	13.7 ± 8.6	17	2.5 ± 0.7	40 ± 10	68 ± 9	24.3	0.15 ± 0.01	3.7
δRzP1-C24U	0.087 ± 0.01	24.6 ± 11.1	4	5.1 ± 1.5	47 ± 8	73 ± 7	530.9	ND	ND

Under single turnover conditions, the cleavage rate (k_2) and the ribozyme concentration at the half velocity (K_m') were determined. Calculated K_d^{P1} values were based on the prediction of thermodynamic stability of the P1 stem duplex (13). K_d^S and K_d^P values were determined using end-labeled uncleavable substrate analogs and synthetic reaction products as described in Materials and Methods.
[a]Kinetic parameters were determined using end-labeled SU8G-9mer.
[b]The magnesium requirement could not be obtained by fitting the experimental data to the least squares equation.
ND represents non-determined values.

cleavage rate (k_2), as well as equilibrium substrate and product dissociation constants (K_d^S and K_d^P) were measured for a *trans*-acting antigenomic *delta* ribozyme and its derived variants.

Product formation or the chemical cleavage step (δRz·S ↔ δRz·P2 + P1)

Wild-type *delta* ribozyme and its variants exhibited various cleavage extents and specificities against the collection of substrates examined. Therefore, we used the complementary pairs of substrates and ribozymes for all subsequent kinetic studies. The cleavage reactions were carried out under standard cleavage conditions described in Materials and Methods. The time courses of substrate cleavage by *delta* ribozyme variants were compared with that of the wild-type (Fig. 3). In these experiments trace amounts of substrate and 500 nM ribozyme were used. We observed both different extents of cleavage and different observed rates of cleavage. δRzP1.1 and δRz P1-A23U exhibited similar observed rates of cleavage (0.25 min^{-1}), but δRzP1-A23U was found to have a higher extent of cleavage (Fig. 3A). Similar findings were observed for δRzP1-C24A and -C24G as compared with the wild-type ribozyme (Fig. 3B). δRzP1-A23G and -C24U cleaved their compensatory substrates 6 and 4 times less efficiently than δRzP1.1, respectively. Within 20 min, all ribozymes had reached their maximum cleavage extent. Various ribozyme concentrations were then used to obtain the experimental data required for the calculation of apparent K_m (K_m') and apparent k_2 values (Table 2). In general, the mutations at either A23 or C24 reduced the rate, resulting in 2- to 6-fold lower k_2 values, but diversely affected the K_m' values. For example, the substitution of A or G at C24 resulted in ribozymes (δRzP1-C24A and -C24G) with similar k_2 (~0.3 min^{-1}), but different K_m' values (102 nM for δRzP1-C24A and 14 nM for δRzP1-A24G). As a consequence, the apparent second-order rate constants, which could be considered as a lower limit for substrate association, varied from 19 $\mu M^{-1}\cdot min^{-1}$ for the wild-type to 4 $\mu M^{-1}\cdot min^{-1}$ for δRzP1-A23G and -C24U, to 76 $\mu M^{-1}\cdot min^{-1}$ for δRzP1-A23U.

Under the standard assay conditions, we observed a decrease in k_2 values with most of the mutants. To verify whether higher magnesium concentrations could restore the lost activity, we determined the magnesium requirements of the wild-type and variant ribozymes as described previously (1; Table 2). We found the K_{Mg} values, the concentration of magnesium at half-maximal velocity, to be ~2 mM for most ribozymes. The mutations which replaced the purine (A) by the other purine (G) at position 23 (δRzP1-A23G) and the pyrimidine (C) by the other pyrimidine

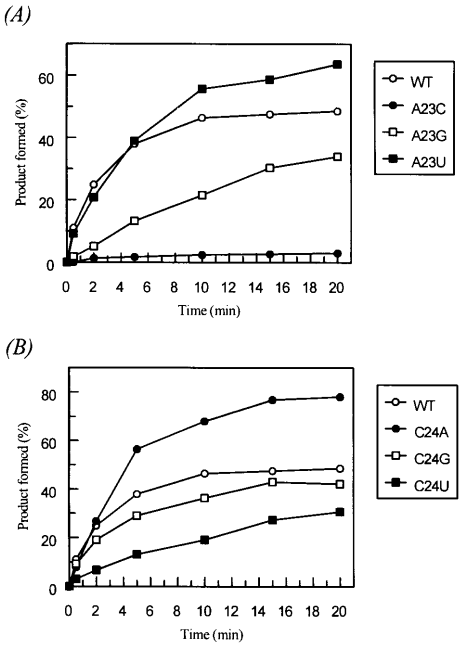

Figure 3. Kinetics of cleavage reactions catalyzed by *delta* ribozymes. Time course cleavage experiments of the wild-type and variant ribozymes under the standard assay conditions described in Materials and Methods. The values for the δRzP1-A23N variants are presented in (**A**) and those for the δRzP1-C24N variants are presented in (**B**). Symbols indicating the plots for δRzP1.1 and the variants are listed in the square inset. The values were averages calculated from two independent experiments.

(U) at position 24 (δRzP-C24U) increased the magnesium requirement ~2-fold (Table 2). Under the standard assay conditions (10 mM Mg^{2+}), δRzP1-A23G has a k_2 value of 0.06 min^{-1}. However, at a higher concentration of Mg^{2+}, we observed that its maximum observed cleavage rate was increased to 0.15 min^{-1}. δRzP1-C24U, whose Mg^{2+} requirement is 5.1 mM, was found to have a k_2 value at higher Mg^{2+} concentrations of 0.11 min^{-1}. The cleavage activity of δRzP1-A23C increased when the $MgCl_2$ concentration was <25 mM and decreased dramatically at $MgCl_2$ concentrations >100 mM (data not shown).

Substrate association and dissociation step (δRz + S ↔ δRz·S)

Equilibrium substrate dissociation constants were measured in order to determine how the variants interact with their substrates. The six variants containing a single mutation at either A23 or C24 can form conventional base pairs with their respective substrates, resulting in the P1 stem of the pseudoknot-like structure (5). Most ribozyme variants exhibited similar K_d^S values of ~30 nM, although the calculated K_d values based on the P1 stem duplex were different (Table 3). Higher K_d^S values were observed for δRzP1-A23U (113 nM) and -C24A (164 nM).

Table 3. Comparative analyses of the thermodynamic parameters affected by the P1 stem mutations

Ribozyme	[a]ΔG°_{P1}	[b]$\Delta G_{E\cdot S}$	[c]$\Delta G^\ddagger$	[b]$\Delta G_{E\cdot P}$
δRzP1.1	-10.7	-10.64	18.8	-10.5
δRzP1-A23C	-12.6	-10.56	19.6	-10.4
δRzP1-A23G	-12.6	-10.56	19.4	-10.1
δRzP1-A23U	-10.7	-9.85	19.2	-11.0
δRzP1-C24A	-8.7	-9.63	18.9	-8.9
δRzP1-C24G	-10.8	-10.49	19.1	-10.2
δRzP1-C24U	-8.9	-10.39	19.5	-10.1

A standard state of 1 M free substrate and ribozyme at 310.15 K (37°C) is assumed to be the same for all *delta* ribozymes. Gibbs energy changes in units of kcal·mol^{-1} are presented.
[a]ΔG°_{P1} is the calculated value for the P1 stem duplex (13).
[b]The free energy of the enzyme–substrate complex ($\Delta G_{E.S}$) and reaction product–ribozyme complex ($\Delta G_{E.P}$) were calculated from the K_d^S and K_d^P, respectively (as listed in Table 2), using the equation $\Delta G_{E\cdot S} = -RT\ln K_d$.
[c]Transition energy ($\Delta G^\ddagger$) was calculated from k_2 using the equation $\Delta G^\ddagger = -RT\ln k_2 \cdot h/k_B \cdot T$. *R*, molar gas constant; *h*, Planck constant; k_B, Boltzman constant.

The substrate association and dissociation constants (k_1 and k_{-1}) for the wild-type ribozyme were determined using a combination of active and inactive ribozymes for determination of the k_{-1} values as described in Materials and Methods. The substrate molecules that dissociate from the inactive ribozyme (A47)–substrate complex are cleaved by the excess active wild-type ribozyme (δRzP1.1) added during the chase period. We used non-denaturing gel electrophoresis to confirm that no alternative complex was present when the inactive and active ribozymes were mixed with the trace amount of substrate. The inactive ribozyme was shown to lack cleavage activity (unpublished data). Although the substrate binding affinity of the inactive ribozyme might be different from that of the active ribozyme, its use provided us with the lower limit for k_{-1} as determined by this method. Since we detected no alternative band in the non-denaturing gels, presumably due to their equivalent masses, we assumed that the observed value was reliable. We could measure the k_{-1} value of 0.13 ± 0.5 min^{-1} independent of either the substrate or the ribozyme concentration. Unfortunately, this method could not be used for the determination of k_1. Due to the limitation that the measurement method required sufficient cleavage activity, we could only determine the k_{-1} values for some variants, namely δRzP1-A23U, -C24A and -C24G (Table 2). We observed that δRzP1-C24G, having similar k_2, K_m', K_{Mg} and K_d^S values to those of δRzP1.1, gave k_{-1} values of a similar magnitude (0.13–0.15 min^{-1}). In contrast, δRzP1-A23U and -C24A exhibited k_{-1} of 0.02 min^{-1}, although both have k_2 and K_{Mg} similar to those of the wild-type ribozyme (Table 2).

Product dissociation and association step (δRz·P2 + P1 ↔ δRz + P1 + P2)

Equilibrium product dissociation constants were measured using 5′-end-labeled P2 reaction products (7 nt long; see Table 1 for the sequences). The reaction products (P2) seem to have binding affinities for the ribozymes similar to those of the substrates. The K_d^P values range between 40 and 60 nM for most variants, similar to those measured for K_d^S (Table 2). Higher K_d^P values were measured for δRzP1-C24A, which also exhibited higher K_d^S values. We found that only ~30% of the end-labeled products could bind to the ribozyme and examined whether the low binding capacity of the reaction products and the ribozymes was due to the presence of the phosphate group on the 5′-end of the reaction products. Under similar conditions, 3′-end-labeled (by ^{32}pCp and RNA ligase) reaction products were tested. We did not detect any increase in the binding capacity (data not shown). Unfortunately, due to the low product–ribozyme binding capacity, we could not accurately measure the k_3 and k_{-3} values.

Thermodynamic analysis of *delta* ribozyme variants

The kinetic parameters obtained were used for the calculation of Gibbs free energy with the k_2 values listed in Table 2 being used to calculate the transition state energy ($\Delta G^\ddagger$) and the K_d^S and K_d^P values for the calculations of $\Delta G_{E\cdot S}$ and $\Delta G_{E\cdot P}$ respectively (Table 3). In general, the mutations caused a decrease in substrate–ribozyme binding affinity, even though the potential to form the P1 stem through conventional Watson–Crick base pairs is identical to that in the wild-type situation. The destabilization of the substrate–ribozyme complex was detected for δRzP1-A23U and -C24A complexes with their $\Delta G_{E\cdot S}$ values increasing ~1 kcal·mol^{-1}. The mutations seemed to stabilize the reaction product–ribozyme complex of δRzP1-A23U since the $\Delta G_{E\cdot P}$ value decreased ~0.5 kcal·mol^{-1}, but destabilize the product–ribozyme complex of δRzP1-C24A since the $\Delta G_{E\cdot P}$ value increased ~0.6 kcal·mol^{-1}. We also noted changes in the transition state energy of 0.4–2 kcal·mol^{-1} among the ribozyme variants as compared with that of the wild-type. The calculated free energy therefore suggested that δRzP1-A23U catalyzed the cleavage of its substrate in the most favorable way as compared with all other ribozymes, including the wild-type.

DISCUSSION

Cleavage reactions of ribozyme variants

Previously, we showed that the positions A23 and C24, which are in the middle of the P1 stem of δRzP1.1, might have significant

effect(s) on the cleavage pathway (3). In order to study their effects, we synthesized a collection of 11mer substrates containing a compensatory mutation at position G7 or U8 (Table 1). The SU8N substrates were used in the cleavage assays catalyzed by δRzP1-A23N ribozymes and the SG7N substrates in the assays catalyzed by δRzP1-C24N ribozymes. The mutations at either position SU8 or SG7 were designed to interfere with the formation of the P1 stem between the ribozyme and substrate and ranged in effect from a very mild one on complementary Watson–Crick base pairing to the stronger interfering effect of non-cannonical base pairing. The base pairs between the ribozyme (A23) and the substrate (SU8) will be referred to as A23N–SU8N and those between C24 and SG7 as C24N–SG7N. The position A23 seems to be the more restricted of the two with respect to any mismatches introduced in the substrate. The conventional base pairing, for example A23–SU8 (A:u), A23U–SU8A (U:a), C24–SG7 (C:g) and C24A–SG7U (A:u), yielded the best P1 stem formation when the extent of cleavage was used to score the effect of these mutations (Fig. 2). However the A23C–SU8G (C:g) pairing did not follow the pattern (see below). The wobble base pair between the two partners also resulted in an extent of cleavage similar to that of both A23G–SU8 (G:u) and C24U–SU8 (U:u). Some base pair preferences were detected for these two positions. For example, the wobble base pair (G-U) results in a higher extent of cleavage when the ribozyme possesses the G instead of the U.

The introduction of any mutation might disturb optimal or proper interactions between the ribozyme and its substrate and therefore affect the minimum reaction steps in various ways depending upon how sensitive that position is to structural changes. Comparative analyses were undertaken to decipher the effect of a single mutation introduced into the middle of the *delta* ribozyme P1 stem. Only comparable kinetic parameters measured using the complementary substrate–ribozyme pairs were analyzed (Table 2). In order to comprehend the effect of these mutations clearly, the mutation at each position will be discussed individually.

δRzP1-A23N ribozymes and respective SU8N substrates

The position A23–SU8 has previously been shown to have an important role in cleavage since any mismatches introduced into the substrate at this position resulted in a complete lack of cleavage with a ribozyme binding affinity similar to that of the wild-type substrate (3). One possible explanation might be that the initial step of the *delta* cleavage pathway involves an incomplete base pairing of the P1 stem. In this scenario, the P1 stem contains a weak hydrogen bond, presumably at position A23, which is flanked by three conventional base pairs on the top of the stem and two conventional base pairs plus an additional wobble base pair at the bottom of the P1 stem. This initial affinity with a weak hydrogen bond(s) is subsequently restored to a more stable form of a conventional base pair prior to the chemical cleavage. The formation of both the P1 stem and the proper substrate–ribozyme complex will then result in product formation. We found that δRzP1-A23C could bind its substrate analog and uncleavable mismatched substrates with the same affinity, reminiscent of the situation observed with the wild-type ribozyme (3). The substrate binding affinity of the δRzP1-A23U variant was not compromised by mismatches in its uncleavable substrates (i.e. SP1.1 and SU8C), although it was surprising that it could bind SP1.1 better than its complementary substrate analog.

When the adenine at position 23 was substituted by the other purine (G), the resulting δRzP1-A23G variant exhibited similar K_m', K_d^S and K_d^P values, but showed a k_2 value 6.3 times lower than that of the wild-type ribozyme. We observed that this ribozyme required more magnesium to reach its maximum cleavage rate (0.14 ± 0.01 min^{-1}; Table 2). The calculated free energy levels ($\Delta G_{E\cdot S}$, $\Delta G_{E\cdot P}$ and $\Delta G^{\ddagger}$) were less stable than those of the wild-type and the increased amount of magnesium seemed to stabilize the transition state conformation, lowering the $\Delta G^{\ddagger}$ value by 0.6 $kcal\cdot mol^{-1}$.

The substitution of A23 with pyrimidine bases resulted in two ribozyme variants with quite astonishing characteristics. While the δRzP1-A23C variant was almost inactive, δRzP1-A23U cleaved efficiently. δRzP1-A23C was shown to form an alternative conformation with its 11mer complementary substrate, SU8G. However, SU8G-9mer, for which only one form of substrate–ribozyme complex was detected, could not be efficiently cleaved by δRzP1-A23C. When we measured the cleavage rate (reflecting k_2), we detected that the magnesium requirement of this ribozyme was very different from that of the wild-type and other variants. The optimal $MgCl_2$ concentration was estimated to be 25 mM.

The δRzP1-A23U variant cleaved its substrate with a rate similar to that of the wild-type ribozyme, but has ~4-times less affinity for its complementary substrate as compared with the wild-type substrate–ribozyme complex (Table 2). A higher affinity of δRzP1-A23U for its reaction product, with the K_d^P value being 2 times lower than the K_d^P value of the δRzP1.1 and its product, was detected (Table 2). These kinetic results suggest that δRzP1-A23U alone, among all variants tested, used the most favorable catalytic pathway. Due to the lower $\Delta G_{E\cdot P}$ (–11 $kcal\cdot mol^{-1}$) as compared with $\Delta G_{E\cdot S}$ (–9.8 $kcal\cdot mol^{-1}$), product formation was favorable. Also, this variant kinetically exhibited the highest apparent second-order rate constant (76 $\mu M^{-1}\cdot min^{-1}$; Table 2) and its calculated k_1 value was 0.17 $\mu M^{-1}\cdot min^{-1}$. Therefore, the product formation step is unlikely to be a rate determining step, rather the substrate association step is more likely to be the rate determining step.

δRzP1-C24N ribozymes and respective SG7N substrates

The position C24 has been shown to be important for both the substrate binding and cleavage steps. The substitution of C24 by U gave rise to the variant δRzP1-C24U that could recognize the complementary substrate with the same affinity as the wild-type ribozyme, but cleaved it at a much slower rate. The resulting transition energy was ~1 $kcal\cdot mol^{-1}$ higher than that of wild-type, indicating that the uridine ring could not stabilize the transition conformation as efficiently as the cytosine ring. However, an increase in the Mg^{2+} concentration restored the cleavage rate to approximately one-third (0.1 min^{-1}) of that of the wild-type ribozyme (Table 2). A similar effect was described earlier for δRzP1-A23G, suggesting that there is some change in the chemical environment.

The variants δRzP1-C24A and -C24G could bind their complementary substrates producing less stable substrate–ribozyme complexes as evidenced by the fact that their Gibbs free energy of binding was ~1 $kcal\cdot mol^{-1}$ greater than that of the wild-type ribozyme (Table 3). Interestingly, the destabilization of the substrate–ribozyme complex did not affect the cleavage rate,

although the transition energy increased by ~1.1 kcal·mol^{-1}. These findings suggest that the transition state conformations formed by δRzP1-C24A and -C24G and their substrates differed from that formed by wild-type ribozyme with its substrate. The magnesium requirement remained similar to that of the wild-type ribozyme, indicating that the structures of the complexes are different.

In summary, these mutational studies suggest that the binding and active sites of the *delta* ribozyme are formed in a unique way. Firstly, the substrate and the ribozyme are engaged in the formation of a helix, known as the P1 stem, which may contain a weak hydrogen bond(s). Secondly, a tertiary interaction involving the base moieties in the middle of the P1 stem likely plays a role in defining the chemical environment. As a consequence, the active site might form simultaneously or subsequently to the binding site during later steps of the pathway, possibly including the product formation step. These conclusions are based on the findings that not only the substrate affinity of the ribozyme changed upon point mutation, but so did the cleavage rate. Furthermore, a single mutation in the P1 stem seemed to affect the transition conformation, thereby directing the pathway. In order to confirm this hypothesis regarding the *trans*-acting *delta* ribozyme, more structural studies are required, including the identification of nucleotides involved in this putative tertiary interaction. Similarly, single functional group mutation on hammerhead and hairpin ribozymes was shown to affect their cleavage pathway (14,15). Clearly, more studies are required for a better understanding of the structure and activity requirements of ribozymes.

ACKNOWLEDGEMENTS

This work was supported by a grant from the Medical Research Council (MRC) of Canada to J.P.P. S.A. is the recipient of a post-doctoral fellowship from Natural Sciences and Engineering Research Council (NSERC) of Canada. D.A.L. is the recipient of a pre-doctoral fellowship program from the Fonds de la Recherche en Santé du Québec (FRSQ). J.P.P. is an MRC scholar.

REFERENCES

1 Lazinski,D.W. and Taylor,J.M. (1995) *RNA*, **1**, 225–233.
2 Perrotta,A.T. and Been,M.D. (1991) *Nature*, **350**, 434–436.
3 Ananvoranich,S. and Perreault,J.P. (1998) *J. Biol. Chem*., **273**, 13182–13188.
4 Mercure,S., Lafontaine,A.D., Ananvoranich,S. and Perreault J.P. (1998) *Biochemistry*, **37**, 16975–16982.
5 Perrotta,A.T. and Been,M.D. (1992) *Biochemistry*, **31**, 16–21.
6 Kawakami,J., Yuda,K., Suh,Y.A., Kumar,P.K.R., Nishikawa,F., Maeda,H., Taira,K., Ohtsuka,E. and Nishikawa,S. (1996) *FEBS Lett*., **394**, 132–136.
7 Nishikawa,F., Fauzi,H. and Nishikawa,S. (1997) *Nucleic Acids Res*., **25**, 1605–1610.
8 Fauzi,H., Kawakami,J., Nishikawa,F. and Nishikawa,S. (1997) *Nucleic Acids Res*., **25**, 3124–3130.
9 Ferre-D'Amare,A.R., Zhou,K. and Doudna,J.A. (1998) *Nature*, **395**, 567–574.
10 Perreault,J.P. and Altman,S. (1992) *J. Mol. Biol*., **226**, 399–409.
11 Hertel,K.J., Herschlag,D. and Uhlenbeck,O.C. (1994) *Biochemistry*, **33**, 3374–3385.
12 Fedor,M.J. and Uhlenbeck,O.C. (1992) *Biochemistry*, **31**, 12042–12054.
13 Serra,M.J. and Turner,D.H. (1995) *Methods Enzymol*., **259**, 242–261.
14 Baidya,N. and Uhlenbeck,O.C. (1997) *Biochemistry*, **36**, 1108–1114.
15 Shippy,R., Siwkowski,A. and Hampel,A. (1998) *Biochemistry*, **37**, 564–570.